

Experimental Investigations on Journal Bearing using SAE 30 and Ferrofluid Lubricants

B. Vijaya Krishna ¹, N. Seetharamaiah ², L. Siva Rama Krishna ³

¹ Research Scholar, ² Professor, ³ Professor,

^{1,3} Department of Mechanical Engineering, University College of Engineering, Osmania University,

² Department of Mechanical Engineering, GITAM School of Technology,
Hyderabad, Telangana, India.



Published in IJIRMPS (E-ISSN: 2349-7300), Volume 11, Issue 4, (July-August 2023)

License: [Creative Commons Attribution-ShareAlike 4.0 International License](https://creativecommons.org/licenses/by-sa/4.0/)



Abstract

The journal bearing test rig is used for experimental research to evaluate the effect of various speeds and loads utilizing two distinct fluids, SAE 30 and Ferro Fluid. The effect of lubricant mobility on a loaded journal bearing is investigated, and metrics such as coefficient of friction, load capacities, and bearing pressure are calculated to better understand the nature of both lubricants. Three distinct loads are introduced to the setup at three different rpms: 500, 600 and 700. A thorough tabular form is created to compare each load bearing capacity. The comparison results suggest that a proper ratio of nano particles added to a lubricant can boost load bearing ability and might carry away most of the temperature created due to friction.

Keywords: Journal Bearing, SAE 30, Ferrofluid

1. Introduction

A journal is known as machine component which upholds another machine component which is known as bearing. It manages the movement between the contact surfaces of the individuals, while conveying the heap. Because of the general movement between the interlinked surfaces, a specific measure of force is gone futile in defeating frictional opposition and in the event that the scouring surfaces are in direct contact, there will be quick wear. To lessen frictional opposition and wear and at times to divert the intensity created, a liquid known as lubricant might be used. The lubricant used to isolate the journal and bearing is typically a refined mineral oil from petrol, likewise vegetable oils, silicon oils, lubes and so on, can be utilized. f all plain bearings, journal bearings are the most popular. It is made up of a sleeve with a shaft rotating inside of it and a thin lubrication coating preventing further contact. They are used in almost all types of hardware and are very common design components.

Any mechanical equipment's performance may be evaluated using a test rig. This experimental setup can be used in labs to find the important parameters like pressure distribution, coefficient of friction, critical pressure, Sommerfeld number and heat generated and dissipated by the bearing. Journal bearing has its wide range of utilities in different sectors of engineering. The bearing that is guiding the shaft has to be strong, load-bearing, and have appropriate thermal qualities. To obtain excellent power transfer, there should be less friction between the bearing and the shaft. Since it will harm both the sleeve and the shaft,

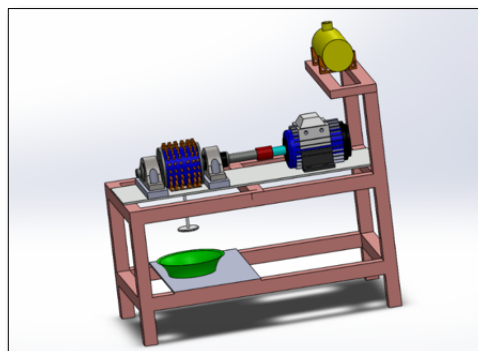
it is best to avoid making direct contact between the two. Between the moving surfaces, a thin lubrication coating is produced to lessen friction. According to the pressure distributions, the load capacities in the journal fluctuate. Higher bearing load causes the shaft and sleeve to come into close contact with one another, damaging both surfaces. To prevent damage to the bearing, the maximum pressure for each bearing should be established such that it never exceeds the limitations when operating.

Laboratory apparatus was created in this effort to ascertain the varied journal bearing settings at various RPMs and load circumstances. The designed experimental apparatus can be setup in any labs without any disruption between the shaft and motor. To begin with the design, analytical calculation is done by performing an experiment on an existing equipment. Later, the setup's component elements are designed. The work includes a planned methodology between hypothetical computation and iterative steps towards design and doable arrangement to test journal bearing apparatus. A detailed tabular methodology is followed to note down the observation values for practical calculations. The values are represented in a graphical format for understanding the variation in pressure distribution due to load varying capacities. A prototype model is fabricated to demonstrate the designed test rig which is built on Solid Works design software.

2. Methodology

Design of journal bearing test rig, is carried out using reverse engineering process by referencing stranded text books and math calculations are performed to calculate diameter of the journal, bearing width, radial clearance and power required for variable speed motor. The making of real time test rig is carried out to test two different oils such as SAE 30 oil and nanofluid (Ferro Fluid under 15% concentration). The design is carried out using solid works and fabrication is done with respective to design.

Figure 1: Final Model of Test Rig in Solid Works



2.1. Experimental Approach

Figure 2: Experimental Flow Chart

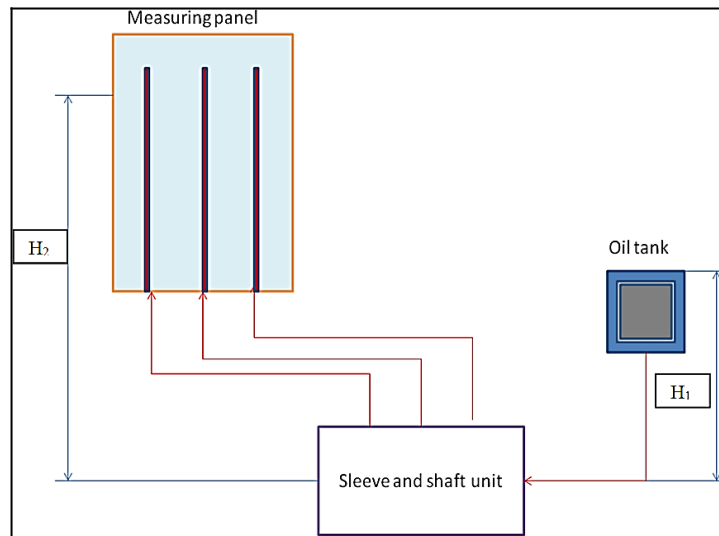


Figure 3: Fabricated Test Rig



2.2. Specifications

- Diameter of the journal = $2r = 55$ mm,
- Diameter of bearing (with 16 radial tapings) = $2r = 70$ mm,

- Bearing width (L) = 15 mm,
- Radial clearance (c) = 3 mm = 0.0025 m,
- Weight of the bearing with attachment = 1.7 Kg,
- DC Motor = 0.5 Hp, 1500 rpm variable speed,
- Dimmer stat is provided for speed variations (Varied from 100 to 120),
- There is a manometer board with 16 tubes, an appropriate scale, and an adjustable oil tank.
- Oil used by us for experiment is SAE 30 lubricating oil.
- Power supply required is AC, 1 Hp, 230 v, stabilized.
- Experiment conducted on Journal Bearing Test Rig.

2.3. Experimental Procedure

Fill the oil tank to the necessary level with the SAE 30 lubricating oil that is being tested (up to 1.5 litre oil). Manometer tubes should all be drained of air before using a supply level indicator to verify level balance. Verify whether there is any oil leaking. For cooling purposes, oil leakage from the sleeve is essential. While increasing the motor's speed, monitor the shaft's speed. Once the oil in the bearing has warmed up, set the speed and let the journal run for about 30 minutes. Then, verify the steady oil levels at different tapings. To maintain the horizontal level positions, add required loads and adjust the balancing weight on the road. Once the manometer values have stabilised, for circumferential and axial pressure distributions take the pressure distributions readings on manometer tubes. Try it again with different loads and speeds. Set the dimmer to zero and turn the main supply off when the test is finished. Maintain the oil tank in the lowest position possible to prevent leaks during the idle period. Loads such as 100 gm, 150 gm, 200 gm, and RPMs 500, 600, 700. The dimmer stat is at 100.

2.4. Calculations

The maximum pressure (Pa - Ps) is occurred at radial angle i.e., 70.1 cm.

2.4.1. Finding Length of the Bearing

Diameter of the journal (d) is 55 mm

We know from design values of journal bearing, the ratio of $\frac{l}{d}$ for journal varies from 1 to 2.

Let's us take $l/d = 1.6$.

$$l = 1.6 d = 1.6 \times 55 = 88 \text{ mm}$$

2.4.2. Bearing Pressure

$$P = \frac{w}{l \cdot d} = \frac{20.59}{88 \times 55} = 0.004254132 \text{ N/mm}^2$$

Note: Load on the bearing:

Total load on the bearing at N rpm = Dry weight of bearing + Weight of the balancing load + Weight added

$$= 1.7 + 2 \times 0.150 + 0.10$$

$$= 2.1 \text{ Kg} = 20.59 \text{ N}$$

2.4.3. Bearing Modulus

Absolute viscosity of SAE 30 oil at temperature 38° C is taken from Table 2,

Absolute viscosity (Z) = 0.078,
and $N = 500$ rpm,
 $P = 0.004254132 \text{ N/mm}^2$,

Therefore, $\frac{zN}{p} = \frac{0.078 \times 500}{0.004254132} = 9167.55$

$$\frac{zN}{p} = 9.16 \times 10^3$$

We consider the operating value from Table 3,

$$\frac{zN}{P} = 28$$

The lowest bearing modulus at which the oil film will facture is obtained by:

$$3k = \frac{zN}{P}$$

In light of this, Bearing Modulus at Minimum Friction,

$$k = \frac{1}{3} \left(\frac{zN}{p} \right) = \frac{1}{3} \times 28 = 9.33$$

The bearing will operate under hydrodynamic conditions, when the calculated value of the journal bearing characteristic number is above 9.00.

Clearance ratio from Table 3: $(c/d) = 0.0013$

From our specifications,
clearance ratio, $(c/d) = 3/55 = 0.0545$

2.4.4. Coefficient of Friction

$$\mu = \frac{38}{10^8} \left(\frac{zN}{p} \right) \left(\frac{d}{c} \right) + k$$

Where, bearing characteristic number (Z) is in kg/m-s,
bearing pressure (P) is in N/mm²
 k = factor to correct for end leakage.

The ratio of the bearing's length to its diameter determines the end leakage factor (k). (i.e., l/d).
 $k = 0.002$ for l/d ratios of 0.75 to 2.8,

$$\mu = \frac{33}{10^8} (9.16 \times 10^3) \left(\frac{1}{0.0545} \right) + 0.002$$

$$\mu = 0.0658.$$

2.4.5. Sommerfeld Number

$$\text{Sommerfeld number} = \frac{zN}{p} \left(\frac{d}{C} \right)^2,$$

For design purpose, its value is taken as

$$\frac{zN}{P} \left(\frac{d}{c} \right)^2 = 14.3 \times 10^6$$

But for $ZN/P = 9.16 \times 10^3$ and $(d/c) = 1/0.0545$ we get,

$$\text{Sommerfeld number} = 30.83 \times 10^5$$

2.4.6. Heat Generated in the Bearing

$$Q_g = \mu w v \text{ watts } \vee N - m/s$$

Where, $\mu = 2.17882 \times 10^{-3}$, and

W = load on the bearing in N,

= bearing pressure in $N/mm^2 \times$ area of the bearing in $mm^2 = p (l \times d)$

$$W = P(l \times d)$$

$$W = 0.004254132 (88 \times 55) \times 9.81 = 20.5899 \text{ N.}$$

and v = rubbing velocity in $m/s = \frac{\pi d N}{60}$

$$V = \frac{\pi \times 0.05 \times 500}{60} = 1.308$$

Therefore, $Q_g = 2.17882 \times 10^{-3} \times 20.5899 \times 1.308 = 17.38$ watts or $N \cdot m/s$

2.4.7. Heat Dissipation

$$Q_d = C \times A (t_b - t_a) \text{ J/s or W}$$

Where C = heat dissipation coefficient in $W/m^2/^\circ C$,

A = Area of the bearing in $m^2 = l \times d$,

t_b = Bearing surface temperature in $^\circ C$, and

t_a = Temperature of the surrounding air in $^\circ C$,

Average value of C is considered as:

For unventilated bearings (still air): 140 to 420 $W/m^2/^\circ C$

For well ventilated bearings: 490 to 1400 $W/m^2/^\circ C$,

Since our bearing is well ventilated bearing, we take the value as 1232,

$$Q_d = c \times l \times d (t_b - t_a)$$

$$Q_d = 140 \times 0.08 \times 0.05 (39 - 29)$$

$$Q_d = 6.16 \text{ watts}$$

2.4.8. Critical Pressure of the Bearing

Critical pressure or minimum operating pressure is,

$$p = \frac{zN}{4.75 \times 10^6} \left(\frac{d}{C} \right)^2 \left(\frac{l}{d+l} \right) \text{ N/mm}^2$$

$$p = \frac{0.078 \times 500}{4 \cdot 75 \times 10^6} \left(\frac{1}{0.0545} \right)^2 \left(\frac{88}{55+88} \right) \text{ N/mm}^2$$

$$p = 1.7010 \times 10^{-5} \text{ N/mm}^2.$$

Similarly, the experiments are conducted for 600 and 700 RPMs for loads 100 gm, 150 gm, 200 gm.

Below table shows the calculated values of design parameters for different loads such as 100 gm, 150 gm, 200 gm, and RPMs 500, 600, 700.

2.5. Results and Discussions

Pressure increases in the system when the load is added. The difference in pressure distributions defines that for different loads and RPMs the performance of the bearing changes. The change in usage of lubricant from SAE 30 to Nano-particle Ferro Fluid has displayed major changes in the heat dissipated section of the experiment.

Table 1: Experimental Readings at Load of 100 kg and 500 rpm Speed

S. No.	Radial Pressure Point (Tube No.)	Load in Kg (W)	Speed (N) rpm	Ps in cm	Pa in cm	(Pa-Ps) in cm
1	1	100	500	53	113	60
2	2	100	500	53	114	61
3	3	100	500	53	106	53
4	4	100	500	53	75	22
5	5	100	500	53	50	-3
6	6	100	500	53	38.5	-14.5
7	7	100	500	53	43	-10
8	8	100	500	53	15	-38
9	9	100	500	53	6.5	-46.5
10	10	100	500	53	96	43
11	11	100	500	53	103	50
12	12	100	500	53	123	70
13	A	100	500	53	120	67
14	B	100	500	53	92	39
15	C	100	500	53	116.1	63.1
16	D	100	500	53	123.1	70.1

Table 2: Experimental Readings at Load of 100 kg and 500 rpm Speed

S. No.	Radial Pressure Point (Tube No.)	Load in Kg (W)	Speed (N) rpm	Ps in cm	Pa in cm	(Pa-Ps) in cm
1	1	100	500	40	54	14
2	2	100	500	40	60	20
3	3	100	500	40	65.5	25.5
4	4	100	500	40	54	14
5	5	100	500	40	50.5	10.5
6	6	100	500	40	50.5	10.5
7	7	100	500	40	48.5	8.5
8	8	100	500	40	46	6
9	9	100	500	40	43.5	3.5
10	10	100	500	40	42	2
11	11	100	500	40	35	-5
12	12	100	500	40	38.5	-1.5
13	A	100	500	40	65	25
14	B	100	500	40	37	-3
15	C	100	500	40	51	11
16	D	100	500	40	62.5	22.5

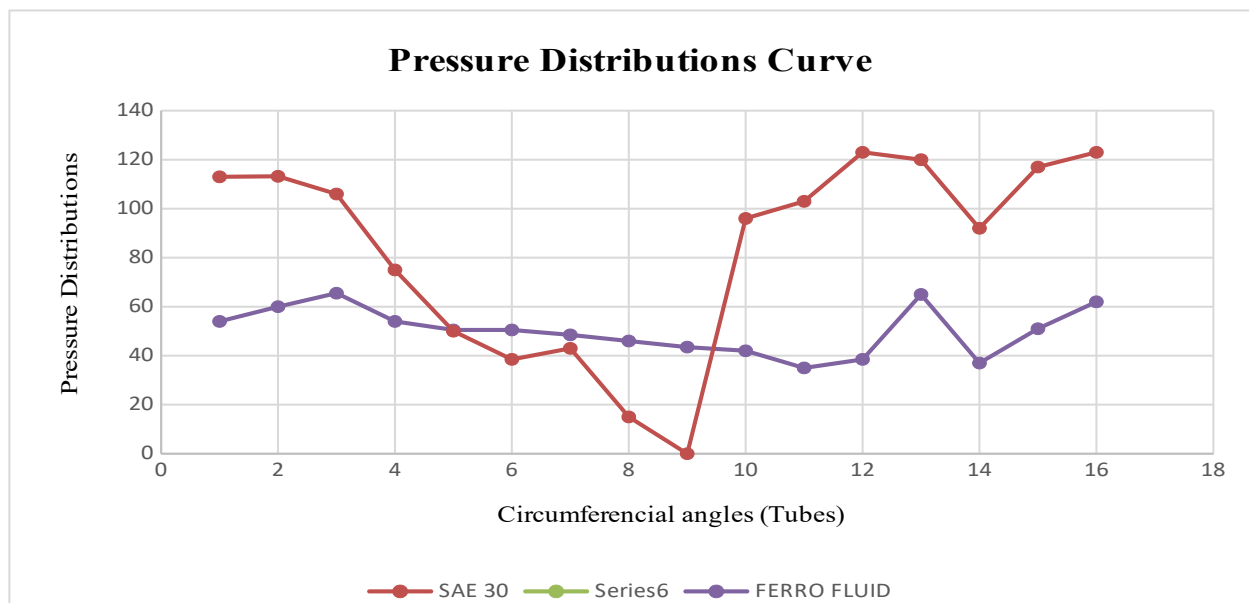
Table 3: Calculated Values of Below Mentioned Parameters at Different Speeds and Loads for SAE 30

(W, N)	l	P	$C = ZN/P$	μ	S	Q_g	Q_d	P
(100, 500)	88	0.004254	9.16×10^3	0.0658	30.83×10^5	17.38	6.16	1.70×10^{-5}
(150, 500)	88	0.004355	6.54×10^3	0.0456	22.01×10^6	12.33	2.4	1.24×10^{-3}
(200, 500)	88	0.004456	5.38×10^3	0.0575	18.1×10^6	15.92	5.12	1.046×10^{-3}
(100, 600)	88	0.004254	5.6×10^3	0.0413	18.9×10^5	13.09	2.24	1.046×10^{-5}
(150, 600)	88	0.004355	4.68×10^3	0.0346	15.7×10^5	11.23	3.6	8.89×10^{-4}
(200, 600)	88	0.004456	3.6×10^3	0.0273	12.2×10^5	9.06	3.2	7.06×10^{-4}
(100, 700)	88	0.004254	3.62×10^3	0.0465	12.18×10^5	16.85	2.8	6.71×10^{-4}
(150, 700)	88	0.004355	3.05×10^3	0.0412	10.28×10^5	15.59	4.2	5.8×10^{-4}
(200, 700)	88	0.004456	2.5×10^3	0.0375	15.54×10^5	14.51	3.84	4.88×10^{-4}

Table 4. Calculated Values of Below Mentioned Parameters at Different Speeds and Loads Ferro Fluid 15% Concentration

(W, N)	L	P	C = ZN/P	μ	S	Q_g	Q_d	P
(100, 500)	88	0.004254	7.0519×10^2	6.91×10^{-3}	23.7×10^4	1.82	3.36	1.30×10^{-6}
(150, 500)	88	0.004355	6.8886×10^2	6.80×10^{-3}	23.19×10^4	1.83	3.361	1.30×10^{-6}
(200, 500)	88	0.004456	6.7324×10^2	6.69×10^{-3}	22.6×10^4	1.85	5.76	1.30×10^{-6}
(100, 600)	88	0.004254	8.4626×10^2	7.09×10^{-3}	28.49×10^4	2.24	2.8	1.57×10^{-4}
(150, 600)	88	0.004355	8.2663×10^2	7.09×10^{-3}	28.5×10^4	2.56	4.2	1.57×10^{-4}
(200, 600)	88	0.004456	8.0789×10^2	7.63×10^{-3}	27.2×10^4	2.52	5.12	1.57×10^{-4}
(100, 700)	88	0.004254	9.8730×10^2	8.88×10^{-3}	33.2×10^4	3.23	2.91	1.83×10^{-4}
(150, 700)	88	0.004355	9.6440×10^2	8.72×10^{-3}	32.4×10^4	3.25	3.6	1.83×10^{-4}
(200, 700)	88	0.004456	9.4254×10^2	8.57×10^{-3}	31.7×10^4	3.26	5.05	1.83×10^{-4}

Figure 4: Pressure Distribution Curve at Circumferential Angles



3. Conclusions

The following conclusions are drawn based on the present analytical and experimental research work:

1. To begin with the process of reverse engineering the load bearing capacities and pressure distributions are taken from the design data book and important parameters are found by performing practical experiment. Sommerfeld's Number and different performance characteristics like bearing modulus, coefficient of friction, heat generate and dissipated are calculated. It is found that for different load capacities we obtain different pressure distributions.
2. Experimental approach has been performed by using two different lubricants SAE 30 and Nano-particle Ferro Fluid. Three different loads 100 gm, 150 gm, 200 gm are added to the setup at three different RPMs 500, 600, 700. A detailed tabular form is recorded comparing each and every load carrying capacity. The results after comparing the obtained values explain that usage of an

appropriate percentage of nano particles in a lubricant can increase the load carrying capacity.

3. After the validation of the two results with analytical and experimental approach a feasible design of the test rig is drawn using Solid Works software. The design dimensions are found with the help of practical calculations. An appropriate test rig is fabricated depicting the designed model. The prototype is presented as a conclusion of the project work.

References

- [1] Patel N.S., Vakharia D.P., Deheri G.M. A study on the performance of a magnetic fluid based hydrodynamic short porous journal bearing. *J Serb Soc Comput Mech*, 2012; 6, 28–44. <https://doi.org/10.5402/2012/603460>
- [2] Hashimoto H. Optimization of oil flow rate and oil film temperature rise in high speed hydrodynamic journal bearings. (In: Dowson D., Taylor C.M., Childs T.H.C., Dalmaz G., Berthier Y., Flamand L., et al., editors. *Tribology for energy conservation*, 34.) Elsevier, 1998, p. 205–10. [https://doi.org/10.1016/S0167-8922\(98\)80075-8](https://doi.org/10.1016/S0167-8922(98)80075-8)
- [3] Myshkin N.K., Goryacheva I.G.. *Tribology: Trends in the half-century development*. *J Frict Wear* 2016, 37. 513–516.
- [4] Peter R.N. Childs. 5 - Journal bearings. (In: *Mechanical Design Engineering Handbook* (2nd ed.), Butterworth-Heinemann, 2019), 167–230. <https://doi.org/10.1016/B978-0-08-102367-9.00005-6>
- [5] Urreta H., Leicht Z., Sanchez A., Agirre A., Kuzhir P., Magnac G. Hydrodynamic bearing lubricated with magnetic fluids. *J Intell Mater Syst Struct*, 2010, 21, 1491–1499. <https://doi.org/10.1177/1045389x09356007>
- [6] Litwin W. Experimental research on marine oil-lubricated stern tube bearing. *J Eng Tribol*, 2019, 233, 1773–1781. <https://doi.org/10.1177/1350650119846004>
- [7] Frene J., Nicolas D., Degueurce B., Berthe D., Godet M. *Hydrodynamic lubrication: Bearings and thrust bearings*. Elsevier, 1997.
- [8] Wardle F. *Ultra-precision bearings*. Elsevier, 2015.
- [9] Bassani R. Lubricated hybrid journal bearings. *J Tribol*, 2011, 133, 1–5. <https://doi.org/10.1115/1.4002875>
- [10] Lampaert S.G.E., Quinci F., van Ostayen R.A.J. Rheological texture in a journal bearing with magnetorheological fluids. *J Magn Magn Mater*, 2020, 499, 1–10. <https://doi.org/10.1016/j.jmmm.2019.166218>
- [11] Glavatskih S., Høglund E. Tribotronics - Towards active tribology. *Tribol Int*, 2008, 41, 934–939.
- [12] Zhu X., Jing X., Cheng L. Magnetorheological fluid dampers: A review on structure design and analysis. *J Intell Mater Syst Struct*, 2012, 23, 839–873. <https://doi.org/10.1177/1045389x12436735>
- [13] Nikolakopoulos P.G., Papadopoulos C.A. Controllable high speed journal bearings, lubricated with electro-rheological fluids. An analytical and experimental approach. *Tribol Int*, 1998, 31, 225–234. [https://doi.org/10.1016/s0301-679x\(98\)00025-5](https://doi.org/10.1016/s0301-679x(98)00025-5)
- [14] Peng J., Zhu K.E.Q. Hydrodynamic characteristics of ER journal bearings with external electric field imposed on the contractive part. *J Intell Mater Syst Struct*, 2005, 16, 493–499. <https://doi.org/10.1177/1045389x05052312>
- [15] Ochoński W. Sliding bearings lubricated with magnetic fluids. *Ind Lubr Tribol*, 2007, 59, 252–265. <https://doi.org/10.1108/00368790710820856>
- [16] Vaz N., Binu K.G., Serrao P., Hemanth M.P., Jacob J., Roy N., et al. Experimental investigation of frictional force in a hydrodynamic journal bearing lubricated with magnetorheological fluid. *J Mech Eng Autom*, 2017, 7, 131–134. <https://doi.org/10.5923/j.jmea.20170705.01>

- [17] Lampaert S.G.E., Ostayen R.A.J. Van. Hydrostatic bearing with MR texturing. In: Book of abstracts: 16th German ferrofluid workshop, 2017, 94–95.
- [18] Kumbhar B.K., Patil S.R., Sawant S.M. Synthesis and characterization of magneto-rheological (MR) fluids for MR brake application. *Eng Sci Technol Int J*, 2015, 18, 432–438.
<https://doi.org/10.1016/j.jestch.2015.03.002>
- [19] Laukiavich C.A., Braun M.J., Chandy A.J. A comparison between the performance of ferro and magnetorheological fluids in a hydrodynamic bearing. *Proc Inst Mech Eng Part J: J Eng Tribol*, 2014, 228, 649–666. <https://doi.org/10.1177/1350650114523753>
- [20] Gertzos K.P., Nikolakopoulos P.G., Papadopoulos C.A. CFD analysis of journal bearing hydrodynamic lubrication by Bingham lubricant. *Tribol Int*, 2008, 41, 1190–1204.
<https://doi.org/10.1016/j.triboint.2008.03.002>